JTTEE5 11:86-94

Peer Reviewed

Evaluation of Four High Velocity Thermal Spray Guns Using WC-10% Co-4% Cr Cermets

Jean-Gabriel Legoux, Bernard Arsenault, Luc Leblanc, Viviane Bouyer, and Christian Moreau

(Submitted 24 October 2000; in revised form 4 January 2001)

Four high velocity thermal spray guns were evaluated in the production of 10% Co-4% Cr tungsten carbide (WC) cermets. Three high velocity oxygen fuel guns (JP-5000, JP-5000ST, and Diamond Jet [DJ]-2700) and one plasma gun (Axial III) were used to spray the same angular, agglomerated, and crushed WC-10Co-4Cr powder. The DPV-2000 was used to monitor the in-flight velocity and temperature of the WC cermet-sprayed particles. From those values, spray conditions were selected to produce coatings that were evaluated in terms of porosity, hardness, and deposition efficiency. Results show that the plasma Axial III provides the highest particle temperature, between 2000 °C and 2600 °C, depending on the spray conditions. The JP-5000 imparts the highest velocity to the particles, between 550 and 700 m/s, depending on the spray conditions. The ST version of the JP-5000 provides the same velocity as the standard version but with lower particle temperature. The DJ-2700 sprays particles with temperature and velocity between those of the JP-5000 and the Axial III. Minimum porosity values of 2.1%, 3.7%, and 5.3%, respectively, were obtained for the JP-5000, the DJ-2700, and the Axial III guns. The porosity and carbide degradation are found to depend mostly on the particle velocity and temperature, respectively. The values for the Vickers microhardness number (200g) ranged from 950 to 1250. Measurements of the deposition efficiency indicated a variation between 10% and 80%, depending on the spray conditions and the gun used.

Keywords abrasion resistance, deposition efficiency, diagnostics, DJ-2700, high power Axial III plasma, JP-5000, JP-5000ST, particle state, porosity, WC-10Co-4Cr

1. Introduction

The development of the high velocity oxygen fuel (HVOF) process has increased the demand for wear-resistant materials. Tungsten carbide (WC)-based coatings are among the most resistant coatings available to sustain various wear conditions such as abrasion, erosion, or sliding.[1] A large variety of metallic matrixes are available to incorporate the WC grains. The best performance in terms of wear resistance is reached with cobalt. Both field trial results and laboratory evaluation results have reported potential corrosion inadequacy of the tungsten carbide cobalt cermets.[2] Synergistic effects have been seen both under salt water and fresh water. On the other hand, the Co-Cr matrix offers a solution for those wet conditions.[3] For this reason, this material is more frequently selected for various applications, such as hydraulic generators, and for chrome replacement applications, such as landing gears.[4]

The continuous evolution of thermal spray techniques has made possible the obtaining of consistent quality coatings from a variety of processes. The selection of a specific process becomes more and more difficult since the available data are generally not generated in the same controlled conditions. The goal in this work was to evaluate four high velocity thermal spray guns, for the production of 10% Co-4% Cr tungsten carbide cermet coatings.

Jean-Gabriel Legoux, Bernard Arsenault, Viviane Bouyer, and **Christian Moreau,** Industrial Materials Institute, National Research Council of Canada, Boucherville, Quebec, Canada; and **Luc Leblanc,** Pyro Genesis, Montreal, Quebec, Canada. Contact e-mail: jean-gabriel.legoux@nrc.ca.

2. Experimental

The coatings were produced under different spraying conditions defined with the aid of the DPV-2000. The same powder was used for all four guns.

2.1 Gun Diagnostics

The DPV-2000 (Tecnar Automation, Lonqueil, Quebec, Canada)[5,6] was used to monitor the velocity and temperature of the in-flight particles using different spray parameters. The values are reported as the average of the measurement on individual particles in the center of the jet. From those values, spraying conditions were selected to produce coatings for further evaluation.

2.2 Thermal Spraying

In this study, three HVOF guns—JP-5000, JP-5000ST (Praxair Tafa, Concord, NH), and Diamond Jet (DJ)-2700 (Sulzer Metco, Westbury, NY)— as well as a plasma gun, Axial III, (Northwest Mettech, Richmond, BC, Canada) were evaluated. The selected parameters for the production of coatings are listed in Table 1. All coatings were produced using an X-Y displacement at constant speed of 0.6 m/s for the Axial III and the two versions of the JP-5000, while a speed of 0.9 m/s was used for the DJ-2700. With respect to the standoff distance (SOD), the JP-5000 was operated at 38 cm, the JP-5000ST at 22.5 cm, the DJ-2700 at 15, 22.5 and 30.5 cm, and the Axial III at 12, 14,

and 16 cm. Step sizes of 5, 3.8, 2.54, and 8 mm, respectively, were used for the JP-5000, the JP-5000ST, the DJ-2700, and the Axial III.

Moreover, a variety of conditions were tested for each gun. For the Axial III gun, seven different spray conditions were tested. The last four (MT4 to MT7) were designed as a Taguchi-type design of experiment (DOE) matrix varying the hydrogen content, the SOD, and the nozzle type. For the JP-5000, complete optimization has already been performed and published elsewhere,[7] so the variations were limited to the kerosene level, the substrate temperature, and the barrel type. Only one coating was sprayed using the JP-5000ST. With the DJ-2700, nine coatings were produced by varying the oxygen, air, propylene, and carrier gas flow rates, as well as the nozzle type, the SOD, and the powder feed rate.

Table 1 Spray Conditions (a)

JP-5000

Sample No.	Kerosene, l/min	Oxygen, SLPM	Barrel Length, cm	Feed Rate, g/min
JP1	0.46	961	10	66
JP2	0.46	961	10	75
JP3	0.38	961	10	75
JP4	0.38	961	20	75
JP5 (ST)	0.19	437	10	75

DJ-2700

Sample No.	Propylene, SLPM	Oxygen, SLPM	Air, SLPM	Carrier Gas, SLPM	SOD, cm	Feed Rate, g/min
DJ1	77	253	384	17.5	22.5	40
DJ2	77	253	384	17.5	22.5	22
DJ3 (a)	77	152	384	17.5	22.5	46
DJ4	85	253	384	17.5	22.5	46
DJ5	85	253	384	17.5	22.5	24
DJ6	77	253	384	12	22.5	24
DJ7	77	253	400	17.5	22.5	24
DJ8	77	253	384	17.5	30.5	24
DJ9	77	253	384	17.5	15	24

Axial III

Sample No.	Nozzle, mm	Total Gas, l/min	Ar, %	N_2, %	H_2, %	SOD, cm
MT1 (b)	7.94	275	75	15	10	14
MT2	7.94	275	75	15	10	14
MT3	7.94	250	75	10	15	12
MT4	7.94	275	70	15	15	16
MT5	7.94	275	80	15	5	12
MT6	9.53	275	70	15	15	12
MT7	9.53	275	80	15	5	16

(a) Barrel 2702 used.
(b) Presence of air jets.

2.3 Materials

An angular agglomerated and crushed WC-10Co-4Cr powder was used. Figure 1 presents the typical aspect of the powder used as well as a cross-section. At the time the study began, it was the only commercially available 10Co-4Cr powder. The particle size distribution was between 15 and 45 μm, with an average size of 30 μm. Since that time, spray-dried powders of various granulometry have become available from most of the materials producers.

2.4 Coating Performance Evaluation

The coatings were evaluated in terms of microstructure, porosity, microhardness, and deposition efficiency. The microstructure and porosity of the coatings were evaluated after proper metallographic preparation involving cutting, vacuum infiltration, and adequate polishing. The porosity level was determined by image analysis of back-scattered electron images. This was performed after calibration of the dynamic range of the microscope imaging system. The development of this technique ensures a precision of 1% on the porosity value. Back-scattered electron images also were used for the qualitative evaluation of carbide degradation. In this case, the presence of dissolved carbides indicated by a large white stringer attesting the presence of tungsten in the solution was used as the main indicator of degradation. Vickers microhardness with a load of 200g was used to characterize the samples. Results are expressed as the mean value of 10 readings. The 200g load was selected to avoid coating cracking or interaction with pores for some samples.

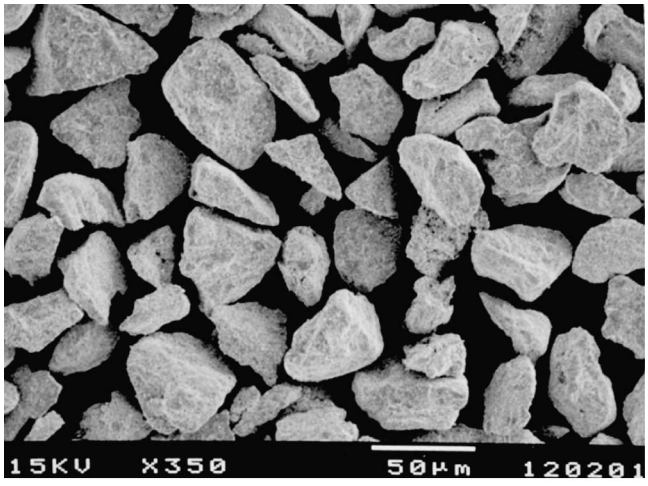

(a)

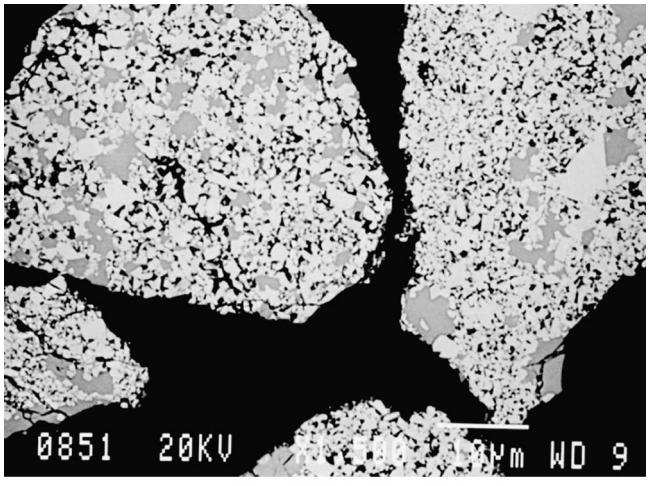

(b)

Fig. 1 WC-10% Co-4% Cr spray powder

Table 2 Properties of the Coatings (a)

Sample	Dep. Efficiency, %	Substrate Temp., °C	Particle Velocity, m/s	Particle Temp., °C	Porosity %	Porosity SD	Hardness VHN	Hardness SD	Volume Loss mm^3	Volume Loss SD
MT1 (b)	86	205	340	2300	6.2	0.6	1082	149	6.2	0.45
MT2	86	170	340	2300	8.6	0.9	1094	184	6.7	0.26
MT3	86	165	320	2350	8.8	1.5	1086	172	7.2	0.68
MT4	84	175	340	2400	5.3	0.5	1066	133	8.7	0.42
MT5	66	140	360	2150	16.1	1.5	949	172	5.6	0.44
MT6	81.5	190	300	2600	6.5	0.5	1059	158	13.7	0.89
MT7	87	155	320	2250	12.6	1.5	1025	149	6.5	0.38
JP1	…	240	…	…	2.1	0.4	1237	134	3.6	0.32
JP2	39	200	665	1805	3.1	0.8	1124	218	2.9	0.14
JP3	31	200	620	1742	2.8	0.6	1213	142	3.2	0.1
JP4	40	200	661	1850	2.7	0.5	1114	95	3	0.32
JP5 (c)	7.8	…	672	1465	0.6	0.1	1206	100	4.2	…
DJ1	…	…	575	1975	5.3	1	1167	178	3.6	0.24
DJ2	…	…	575	1975	3.7	0.8	1201	160	3.3	0.25
DJ3	57	…	562	1840	8.4	1.64	1067	106	3.6	0.03
DJ4	…	…	570	1980	5	0.39	1149	140	3.6	0.13
DJ5	63	…	570	1980	4.6	0.93	1239	139	3.7	0.05
DJ6	62	…	570	2005	4.5	0.39	1156	272	3.9	0.14
DJ7	62	…	570	1975	4.7	0.73	1141	157	3.4	0.12
DJ8	65	…	530	1915	7.7	1.2	1053	172	3.4	0.07
DJ9	67	…	590	2025	5.6	0.91	1214	118	3.9	0.24

(a) Dep.—Deposit; temp.—temperature; VHN—Vickers hardness number.
(b) Presence of air jets.
(c) ST gun used.

2.5 Abrasive Wear

The abrasive wear resistance of the coatings was evaluated according to the ASTM G-65 standard (i.e., for dry sand and rubber wheel). The wear volume loss of the coatings was determined using a laser profilometer according to a technique described previously.[8] The results are presented as the mean value of three abraded sample replicates.

3. Results and Discussion

The results are presented for each gun in terms of particle condition and coating microstructure. A more general comparison of the different coating conditions is given at the end of the Discussion section. Table 2 describes the results obtained for each coating condition.

3.1 Axial III

Profiles of the particle temperature and velocity measured along the gun axis are presented in Fig. 2. The particle temperature ranged between 2000 and 2600 °C, depending on the spray conditions and the SOD. The velocities attained by the particles ranged between 300 and 400 m/s. This velocity range is considerably higher than that obtained using conventional plasma equipment,[9] which is usually below 250 m/s.

The temperature and velocity of the particles decrease continuously from the exit of the gun. The manufacturer-recommended spray distance is 140 mm. The velocity and temperature curves are parallel, however, their relative positions or orders are different. For instance, the MT1 condition yields an intermediate temperature but imparts the highest velocity to the particles. This indicates that temperature and velocity can be controlled independently to some extent.

It can be seen from the properties of the coatings presented in Table 2 that coating microhardnesses are all in the same range. A slightly lower hardness value is obtained for the more porous coating sprayed with the lowest particle temperature.

The coating porosity varied between 5.3% and 16.1%, depending on the spray parameters. For example, the porosity of MT1 is significantly lower than for sample MT2. This reduction can be caused either by the presence of air jets or by the higher surface temperature of MT1 during spraying. It should be noted at this point that the higher substrate temperature was caused by a reduction of the external cooling of samples in an attempt to compensate for the presence of air jets. In conventional plasma spraying, the removals of overspray by the use of air jets during spraying usually leads to less porous coatings. On the other hand, we can find a strong relationship between the coating surface temperature and the coating porosity, as shown in Fig. 3. In plasma spraying, studies have demonstrated the importance of the substrate temperature on the coating quality.[9,10] We also should note that it is difficult to distinguish between the effect of surface temperature and the in-flight particle temperature since they are strongly correlated, as shown in Table 2.

The variations of properties observed among samples MT4 to MT7 can be interpreted by the use of a Taguchi-type approach since they are produced using a saturated L4 matrix design for the experiment. Table 3 presents the summary of the observed effects on the porosity and the particle state. The results are obtained by the computation of the difference between the average value obtained with a parameter set at one condition (designated "+") and the average value with the parameter set at the condition designated "–" in the "Level" column. Thus, a positive value indicates that the condition designated "+" produces the higher result, while a negative value indicates that the condition designated "–" produces a higher result. These results show that the SOD influences the deposition efficiency. In this case, work-

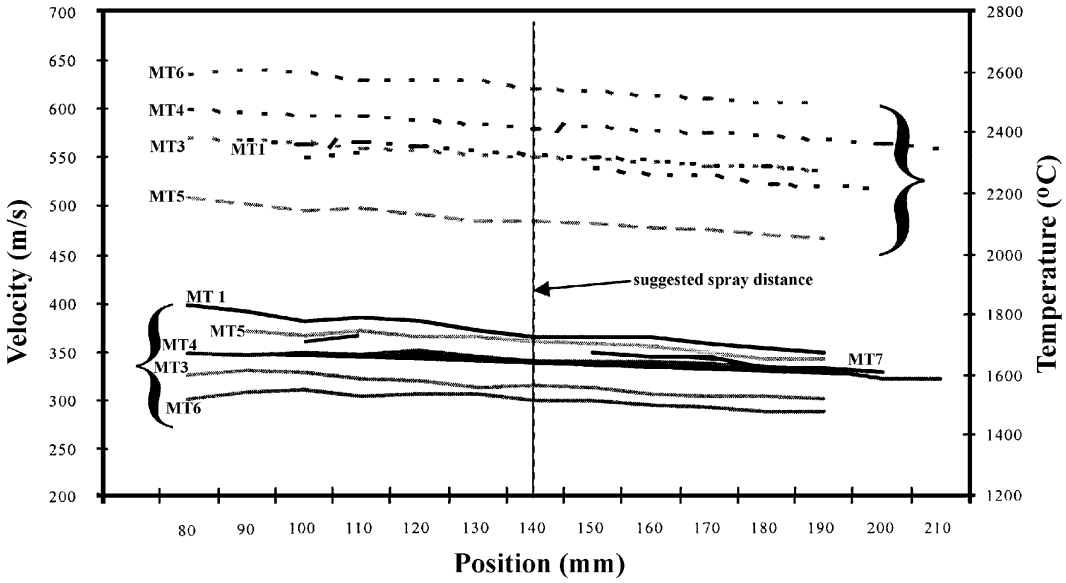

Fig. 2 Axial profiles of particle velocity and temperature for the Axial III gun

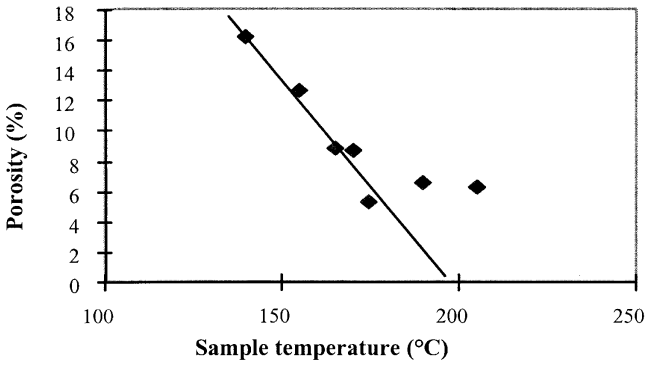

Fig. 3 Porosity-surface temperature relationship for coatings made using the Axial III gun

ing at a longer distance (i.e., 160 mm compared to 120 mm) increases the deposition efficiency. Comparing the effect of hydrogen, the use of 15% instead of 5% increases the substrate and the particle temperatures, but reduces the particle velocity. The porosity level decreases by 8.5% with the use of the high hydrogen content, which is directly related to the increase in the temperature of both the particles and the substrate. Using a smaller nozzle (7.94 mm) increases the velocity of the sprayed particles and decreases their temperature, but it has a marginal effect on the porosity level of the coatings.

Figure 4 presents the typical micrographs of the produced coatings. Samples MT1 and MT2 were produced under the same conditions, but MT1 was produced using air jets and a higher substrate temperature (205 °C). The sample MT1 (Fig. 4a) is less porous than sample MT2 (Fig. 4d). Both samples present good carbide retention with little apparent carbide dissolution. The pores are located preferentially around the solidified droplets. The sample MT5 (Fig. 4b), produced using cool and fast particles, presents almost no carbide degradation but does present a high level of porosity. Figure 4(c) shows the resulting microstructure of sample MT4, produced from fast and hot particles, giving a very dense coating with a significant amount of degraded carbides and also numerous vertical cracks. As seen in Table 2, the presence of the large area depleted in carbides and vertical cracks are more deleterious to the abrasive wear resistance than the presence of pores.

3.2 JP-5000

Extensive optimization of the JP-5000 HVOF gun already has been done in another work;[9] therefore, fewer coatings were produced with this gun.

Figure 5 shows the axial profile of the particle state for both the standard and ST versions of the JP-5000. The JP-5000 gun imparts the highest particle velocity among the guns tested in this study, between 550 and 700 m/s depending on the spray conditions. The ST version of the JP-5000 provides about the same velocity as the standard version but with significantly lower particle temperature. The curves remain in the same relative order when measuring either the velocity or the temperature. The spray conditions producing the highest velocities also yield the highest particle temperatures. All conditions produce similar velocities between the gun and an SOD of 25 cm, after which the velocities start to diverge from one spray condition to another. It can be noted that with the ST version, velocity decreases more rapidly than with the standard version of the JP 5000. However, although the manufacturer-suggested spray distance is 38 cm with the standard gun, it is reduced to 28 cm with the ST version. This recommendation allows the ST version to have particle velocities similar to those of the standard version of the JP 5000 but yields lower particle temperature.

The highest temperature (1850 °C) is obtained with the JP-5000 when using a 20 cm barrel, while the JP-5000ST provides much cooler particles (1500 °C). At the latter temperature, the metallic matrix is not fully melted, which gives rise to a very low deposition efficiency of 7.8%. Nevertheless, the resultant coat-

ing is very dense (Table 2). In an attempt to increase the deposition efficiency, the oxygen and kerosene flow rates were increased to 580 standard liters per minute (SLPM) and 0.25 l/min, respectively. However, even under those extreme conditions for the JP-5000ST, the particle temperature was still lower than 1600 °C (curve JPST*, Fig. 5) and the increased pressure in the combustion chamber leads to very high barrel and electrode wear. This latter condition then was judged nonviable, and no coatings were produced.

The coating JP1 was produced using the same conditions as JP2 but with a higher surface temperature. Increasing the substrate temperature seems to reduce the porosity but also reduces the abrasion wear resistance, a volume loss increase from 2.9 to 3.6 mm^3 in this particular case (Table 2).

Typical microstructures of coatings produced using the JP-5000 are presented in Fig. 6. Both coatings are very dense, but the one from the standard JP-5000 contains more visible pores. In both coatings, no carbide dissolution is observed. All standard JP-5000 coatings exhibit the best abrasion wear resistance compared with those produced with the Axial III and the DJ-2700. As observed previously, the coating performance is not related to the porosity level.

Table 3 Effect of the Axial III Parameters on the Particle State and Coating Properties (Major Effects are Bold) (a)

Parameter	Levels +/−	Deposit Efficiency, %	Substrate Temp., °C	Particle Vel. m/s	Particle Temp., °C	Porosity, %	Hardness, VHN	Volume Loss, mm^3
Nozzle	9.5/8	0.93	−1.5	**−40**	**150**	−1.2	35	2.95
H_2, %	15/5	6.3	**35**	**−20**	**300**	**−8.5**	76	**5.15**
SOD	16/12	**11.8**	0	0	−50	−2.4	42	−2.05

(a) temp.—temperature; Vel.—velocity; VHN—Vickers hardness number.

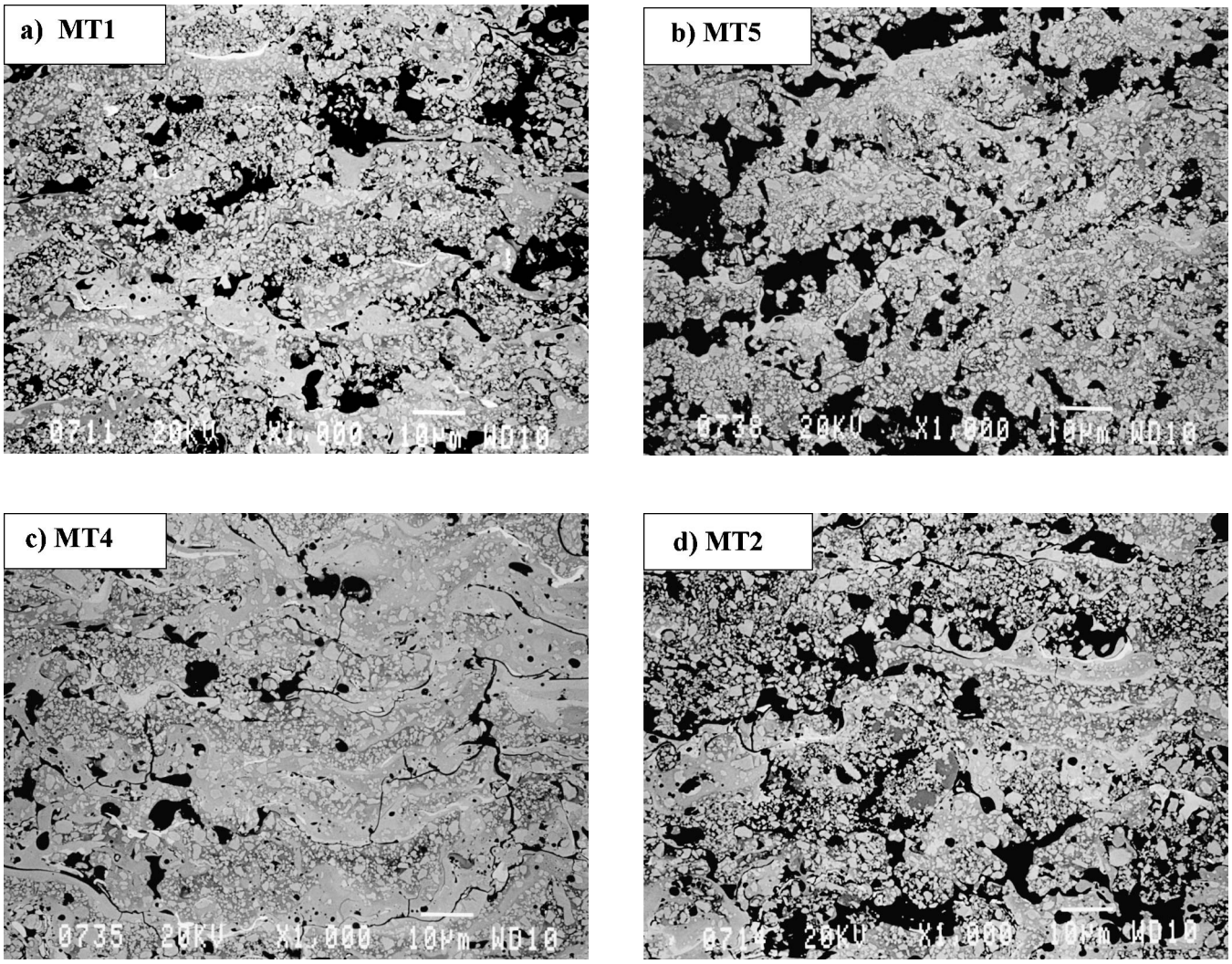

Fig. 4 Microstructure of some Axial III coatings: **(a)** MT1; **(b)** MT5; **(c)** MT4; and **(d)** MT2

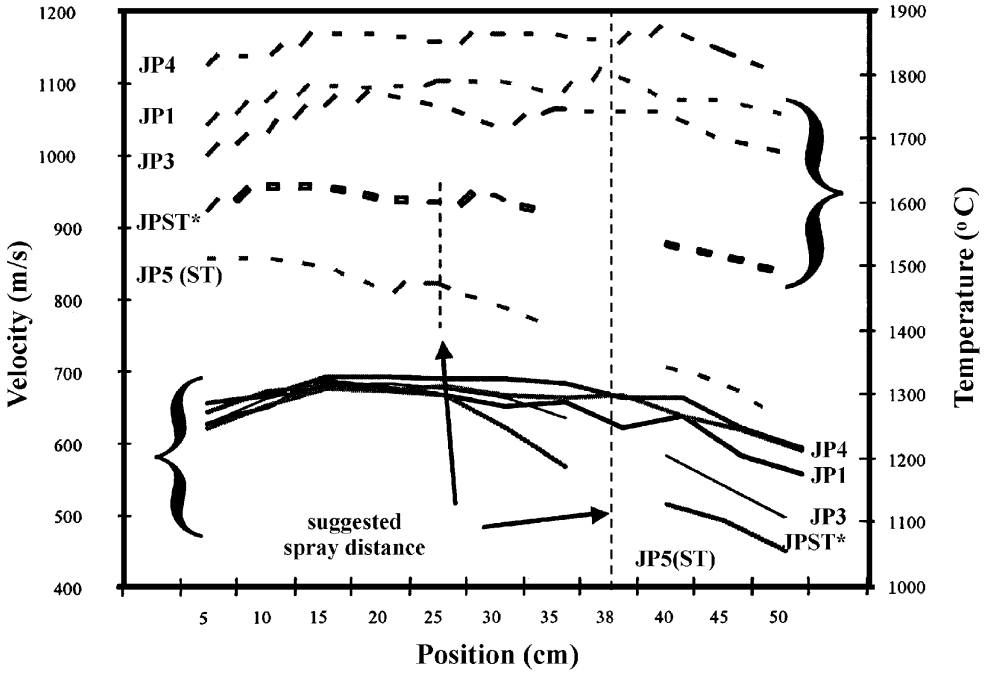

Fig. 5 Axial profiles of particle velocity and temperature for the JP-5000 gun and the JP-5000ST guns

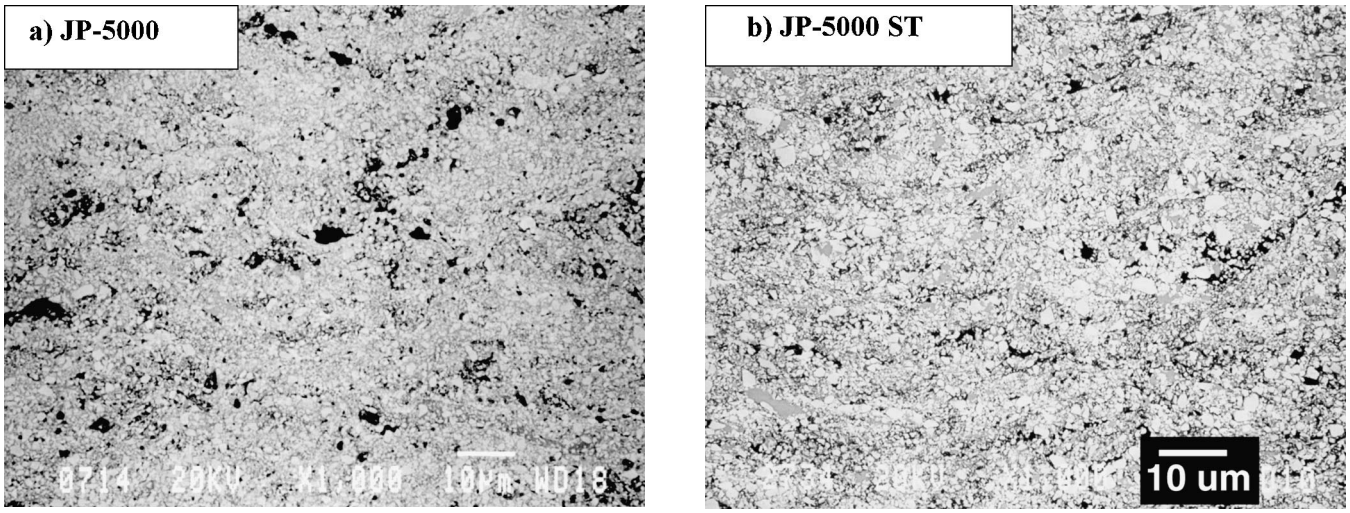

Fig. 6 Microstructure of the coatings produced using **(a)** the JP-5000 gun and **(b)** the JP-5000ST gun

3.3 DJ-2700

Axial profiles of the particle velocity and temperature measurements are presented in Fig. 7. For the sake of clarity, only profiles DJ2 and DJ3 are presented, all the other profiles being in between these two. It can be noted that, similar to the coating profiles of the JP-5000, the temperature and velocity profiles do not decrease from the gun exit. Instead, the particles are accelerated during the first 15 cm from the gun, then continuously decelerate. The temperature and velocity of the particles are intermediate between those of the JP-5000 and the Axial III guns.

The properties of the coatings are detailed in Table 2. The particle velocity varies between 500 and 600 m/s, which is nearly 100 m/s slower than the velocities obtained using the JP-5000. On the other hand, the temperature range obtained using the DJ-2700 is between 1840 and 2025 °C;, which is nearly 200 °C higher than the particle temperature produced with the JP-5000.

Figure 8 presents some of the typical microstructures of the coatings obtained with the DJ-2700. Of particular note is the higher porosity of sample DJ3 (Fig. 8c) and the presence of more carbides dissolved in the form of stringers in samples DJ6 and DJ5 (Fig. 8b and d, respectively).

The coatings sprayed with the DJ-2700 were produced under different spray conditions varying one parameter at a time. The effects of those parameters are listed in Table 4. The results are

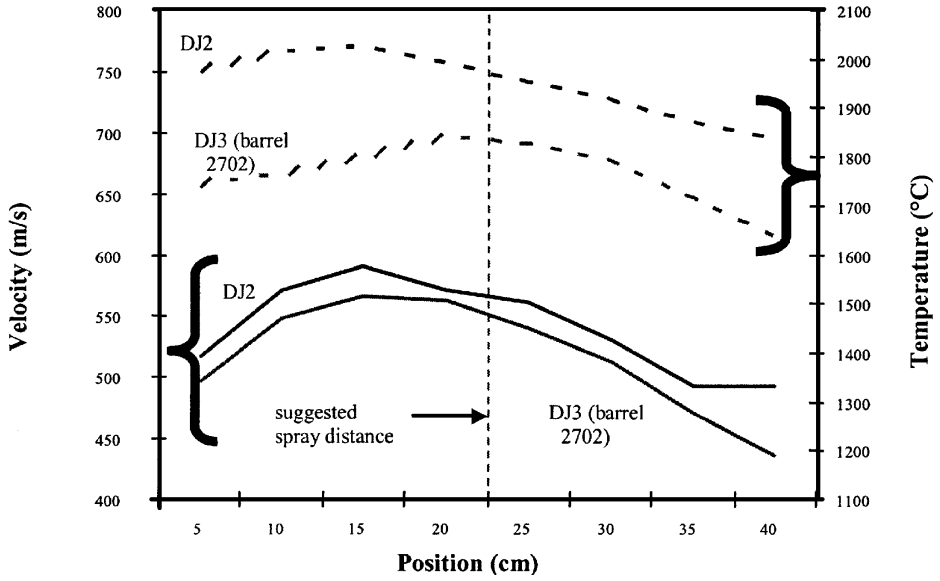

Fig. 7 Axial profile of particle velocity and temperature for the DJ-2700 gun

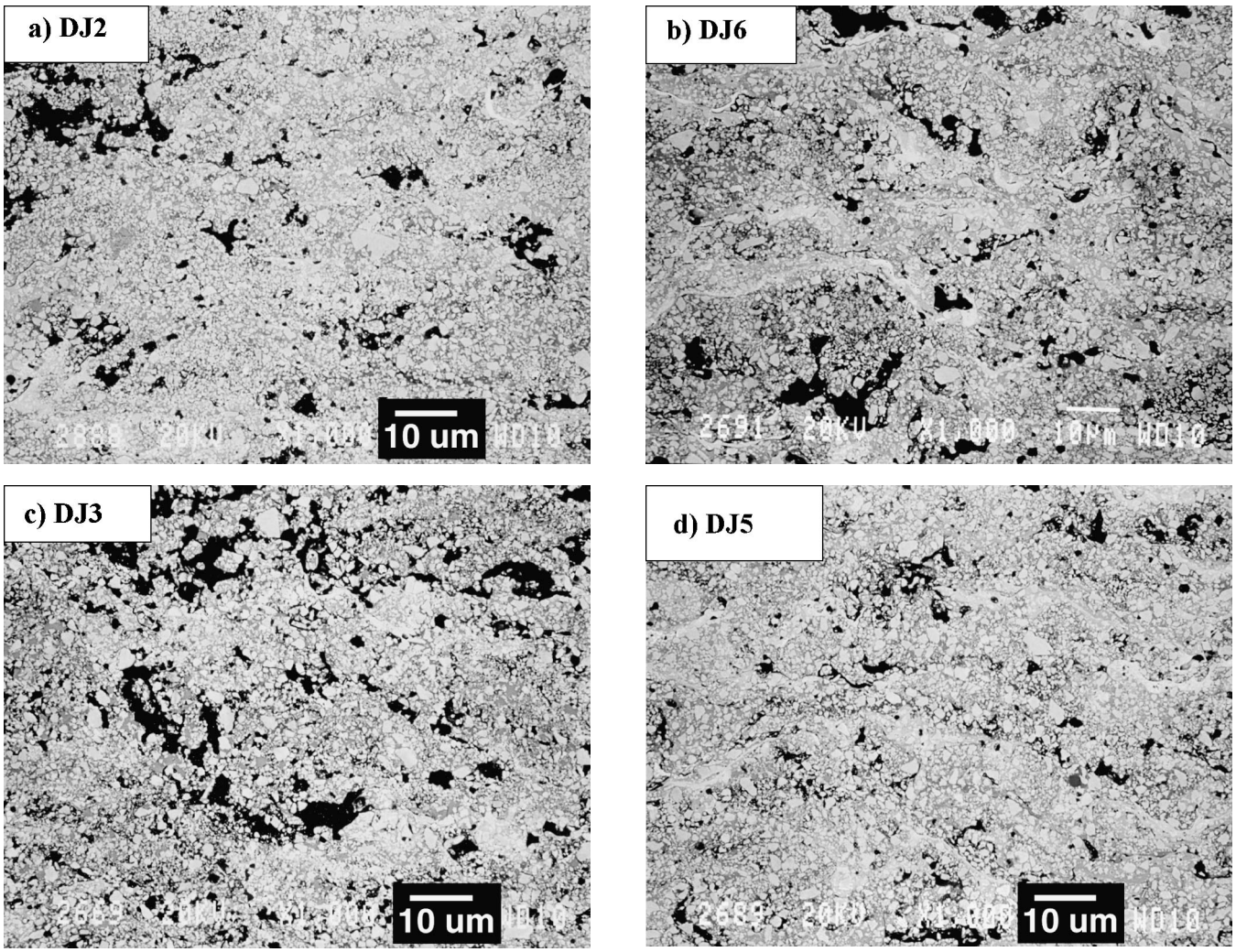

Fig. 8 Microstructure of some Diamond Jet coatings: **(a)** DJ2 (standard conditions); **(b)** DJ6 (low carrier gas); **(c)** DJ3 (using barrel 2702); and **(d)** DJ5 (high propylene flow rate)

obtained by the computation of the difference between the reference condition and the condition having the parameter changed. Thus, a positive value indicates that the reference condition (DJ2) produces the higher result, while a negative value indicates that the condition using the variation of the parameter produces a higher result.

The SOD has the largest effect on the coating properties and the particle state. This can be understood easily by looking at Fig. 7. Indeed, the particle velocity and temperature vary more along the gun axis than between the different spray conditions.

3.4 Relationship Between Coating Characteristics and Particle Velocity and Temperature

Figure 9 shows the observed relationship between the in-flight particle temperature and the abrasive-wear volume loss for the coatings produced using the four different guns. As seen in Fig. 9, the wear resistance appears well correlated with the particle temperature, the abrasion volume loss increasing with the particle temperature. This could be attributed to the higher carbide degradation of the WC at the higher temperature.[11] Further work would be needed such as quantitative x-ray diffraction or the simulation of the thermal history of particles to assess this point in more detail.

Considering the importance of the powder cost, the deposition efficiency is a key factor for the industrial use of these coatings. The low particle temperature has a negative influence on the deposition efficiency, as seen in Fig. 10. Considering the curves of Fig. 9 and 10, it appears that depositing coatings with particle temperatures around 2000 °C would provide a good compromise between the abrasion wear resistance and the cost.

From a more global point of view, if we compare the results obtained from the four guns, we notice a good correlation between the coating porosity and the particle velocity for the three HVOF guns, as is shown in Fig. 11. The coatings produced by the Axial III are less porous than what can be expected only from the tendency observed for the HVOF guns. This appears in agreement with our earlier observations in Fig. 3 for the Axial III gun, where the porosity was mostly influenced by the substrate temperature.

Table 4 Effect of the DJ-2700 Parameters on the Particle State and Coating Properties (Major Effects are Bold) (a)

Parameter	Levels (Sample), +/−	Particle Velocity, m/s	Particle Temp., °C	Porosity, %	Hardness, VHN	Volume Loss, mm^3
Powder feed rate	22/40 (DJ2/DJ1)	0	0	−1.6	34	−0.3
	46/24 (DJ4/DJ5)	0	0	0.4	−90	−0.1
Propylene	176/194 (DJ2/DJ4)	5	−5	−1.3	52	−0.3
Air	876/912 (DJ2/DJ7)	5	0	−1	60	−0.1
SOD	22.5/30.5 (DJ2/DJ8)	**45**	**60**	**−4**	**148**	−0.1
	22.5/15 (DJ2/DJ9)	−15	**−50**	−1.9	−13	**−0.6**
Carrier gas	17.5/12 (DJ2/DJ6)	5	**−40**	−0.8	45	**−0.6**

(a) temp.—temperature; VHN—Vickers hardness number.

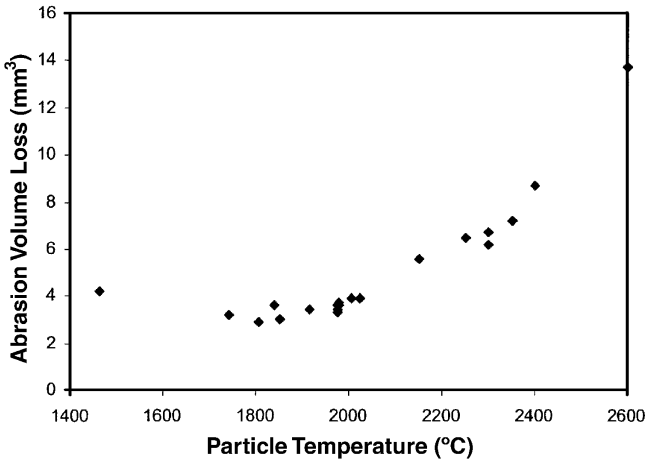

Fig. 9 Abrasion volume loss as a function of the in-flight particle temperature

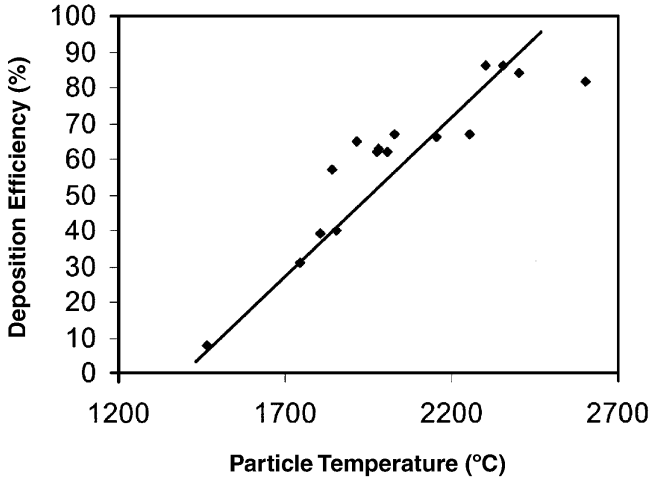

Fig. 10 Deposition efficiency in function of the in-flight particle temperature

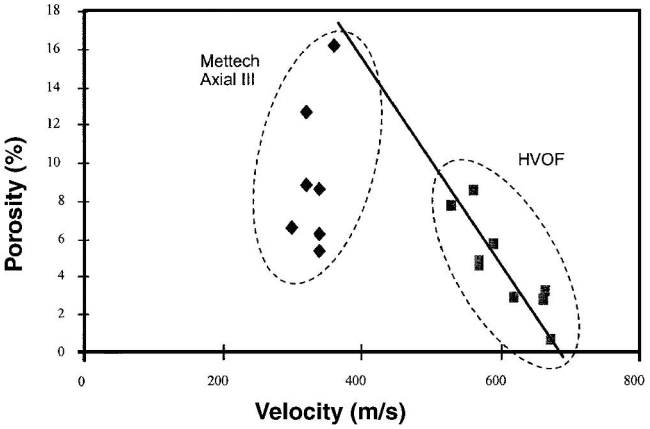

Fig. 11 Coating porosity as a function of the in-flight particle velocity

4. Summary

Three HVOF guns (the JP-5000, JP-5000ST, and DJ-2700) and a plasma gun (Axial III) were evaluated in the production of 10% Co-4% Cr tungsten carbide cermets using the same agglomerated and crushed powder.

Particle state monitoring was performed for each gun under various spray conditions.

- The JP-5000 provides the highest velocity and the lower temperature to the particles.
- The Axial III provides the highest temperature and the lower velocity to the particles.
- The DJ-2700 provides temperature and velocity between those of the JP5000 and the Axial III.

Coatings were evaluated in terms of microstructure, porosity, microhardness, abrasion, wear resistance, and deposition efficiency.

- Minimum porosity values of 2.1%, 3.7%, and 5.3%, respectively, were obtained for the JP-5000, the DJ-2700, and the Axial III guns.
- The values for the Vickers microhardness number (200g) ranged from 950 to 1250.
- Measurements of the deposition efficiency indicated a variation between 10% and 80%, depending on the spray conditions and the gun technology.

The in-flight particle state is related to the coating properties.

- For the HVOF guns, the coating porosity is dependent on the particle velocity, while it is related both to the substrate temperature and the particle velocity for the Axial III gun.
- The abrasion wear resistance and the carbide degradation are related to the particle temperature.
- The deposition efficiency is related to the particle temperature.

References

1. E. Novinski: "Current Status of the Development and Application of Chromium Plating Alternatives Using the HVOF Process," paper presented at the Third Global Symposium on HVOF Coatings, University of Tulsa, March 24, 1997, San Francisco, CA.
2. S. Simard, B. Arsenault, J.G. Legoux, and H.M. Hawthorne: "Erosion/Corrosion of HVOF Coatings," paper presented at Corrosion 99, Nace International San-Antonio, TX, April 25-30, 1999, Conférence Paper 295.
3. T. Rogne, M. Brodal, T. Solem, and E. Bardal: "The Importance of Corrosion on the Erosion-Corrosion Performance of Thermal Spray Ceramic-Metallic Coatings," in *Thermal Spray: Practical Solution for Engineering Problems*, C.C. Berndt, ed., ASM International, Materials Park, OH, 1996, pp. 207-14.
4. B.D. Sartwell and P.E. Bretz: "HVOF Thermal Spray Coatings Replace Hard Chrome," *Adv. Mater. Proc.*, 1999, *156*(2), pp. 25-28.
5. J. Blain, F. Nadeau, L. Pouliot, C. Moreau, P. Gougeon, and L. Leblanc: "An Integrated Infrared Sensor System for On-line Monitoring of Thermally Sprayed Particles," *Surface Eng.*, 1997, *13*, pp. 420-24.
6. C. Moreau, P. Gougeon, M. Lamontagne, V. Lacasse, G. Vaudreuil, and P. Cielo : "On-Line Control of the Plasma Spraying Process by Monitoring the Temperature, Velocity, and Trajectory of In-Flight Particles," in *Thermal Spray Industrial Applications*, C.C. Berndt and S. Sampath, ed., ASM International, Materials Park, OH, pp. 431-37.
7. B. Arsenault, J.G. Legoux, H. Hawthorne, and J.P. Immarigeon: "VOF Process Optimization for the Erosion Resistance of WC-12Co and WC-10Co-4Cr," paper presented at ITSC 2001, Singapore, 2001.
8. S. Dallaire, M. Dufour, and B. Gauthier: "Characterization of Wear Damage in Coating by Optical Profilometry," *J. Thermal Spray Technol.*, 1993, *2*(4), pp. 1-6.
9. M. Prystay, P. Gougeon, and C. Moreau: "Correlation between Particle Temperature and Velocity and the Structure of Plasma Sprayed Zirconia Coatings," in *Thermal Spray: Practical Solutions for Engineering Problems*, C.C. Berndt, ed., ASM International, Materials Park, OH, pp. 517-23.
10. L. Bianchi, P. Lucchese, A. Denoirjean, and P. Fauchais: "Zirconia Splat Formation and resulting Coating Properties," in *Advances in Thermal Spray Science and Technology*, C.C. Berndt and S. Sampath, ed., ASM International, Materials Park, OH, pp. 261-66.
11. L. Jacobs, M.M. Hyland, J. Gutleber, and S. Sampath: "Study of the Decarburation Reactions and Phase Transformations of a WC-Co Powder," in *Proc. United Thermal Spray Conference 99*, E. Lugscheider and P.A. Kammer, ed., DVS-Verlag GmbH, Dusseldorf, Germany, 1999, pp. 439-45.